Research Article

Mohammed Hawash*, Nidal Jaradat, Murad Abualhasan, Johnny Amer, Serkan Levent, Shahd Issa, Sameeha Ibrahim, Aseel Ayaseh, Tahrir Shtayeh, Ahmed Mousa

Synthesis, chemo-informatics, and anticancer evaluation of fluorophenyl-isoxazole derivatives

https://doi.org/10.1515/chem-2021-0078
received May 20, 2021; accepted July 30, 2021

Abstract: The current study aimed to design and synthesize a novel series of fluorophenyl-isoxazole-carboxamide derivatives and evaluate their antiproliferative activities. Anticancer activities of the novel compounds were evaluated by MTS assay against four cancer cell lines, including liver (Hep3B, HepG2), cervical (HeLa), and breast (MCF-7), and α-fetoprotein tumor marker, cell cycle analysis, and annexin V tests. Chemo-informatics analysis showed that all synthesized derivatives **2a–2f** obeyed Lipinski's rule. Compound **2f** was the most potent compound against Hep3B and Hep-G2 cancer cell lines with IC_{50} values of 5.76 and 34.64 μg/mL, respectively. Moreover, compounds **2a–2c** and **2e** showed potent inhibitory activity against Hep3B with an IC_{50} value range of 7.66–11.60 μg/mL. Hep3B secretions of α-fetoprotein (α-FP) results showed that compound **2f** reduced the secretion of Hep3B to 168.33 ng/mL and compound **2d** reduced the secretion to value approximately 598.33 ng/mL, in comparison with untreated cells' value of 1116.67 ng/mL. Furthermore, cell cycle analysis showed that the **2f** compound induced arrest in the G2-M phase in 6.73% of the total cells and that was lower than the activity of the positive control doxorubicin (7.4%). Moreover, **2b** and **2f** compounds reduced the necrosis rate of Hep3B to 4-folds and shifted the cells to apoptosis.

Keywords: isoxazole, anticancer, Hep3B, doxorubicin

1 Introduction

Cancer is a disease that has spread in recent decades, and it is one of the main reasons for mortality and death worldwide [1–3]. In 2016, about 17.2 million new cases of cancer and 8.9 million deaths were registered around the world. From 2006 to 2016, there was an increase in cancer cases of about 28% [4]. However, in 2018, the number of deaths was estimated at 9.6 million, and according to the World Health Organization (WHO), the distribution of the most common cancers was as follows: breast (2.09 million), lung (2.09 million), colorectal (1.80 million), prostate (1.28 million), and skin cancer (1.04 million) [3].

Hepatocellular carcinoma (HCC), the fourth most common type of cancer, was one of the leading causes of cancer-related deaths in 2020. Approximately 80% of cases found in Asia and the African regions arise due to hepatitis B, C, and chronic alcohol use. The early stage of HCC is asymptomatic and the patients are diagnosed in the advanced stages. Surgical therapy was associated with post-operative complications and a high risk of recurrence. Radio-frequency ablation, microwave ablation, radioembolization, molecular targeted therapies, and chemotherapy remain the alternative ways of treatment [5,6].

Cancer occurs due to the abnormal and uncontrolled proliferation of living cells and damage of the genes that regulate the cell cycle [7]. The cancer therapy protocols include surgery, radiation, immunotherapy, gene therapy, and chemotherapy. Nowadays, chemotherapy is an effective way to stop and eliminate cancer growth. New methods of treatment depend on mechanisms involved in cancer progression [3,8].

Chemotherapy has been widely used, particularly against various cancer types [9]. However, many agents

* **Corresponding author: Mohammed Hawash,** Department of Pharmacy, Faculty of Medicine and Health Sciences, An-Najah National University, P.O. Box 7, 00970, Nablus, Palestine, e-mail: Mohawash@najah.edu, tel: +972-569-939-939
Nidal Jaradat, Murad Abualhasan, Shahd Issa, Sameeha Ibrahim, Aseel Ayaseh, Tahrir Shtayeh: Department of Pharmacy, Faculty of Medicine and Health Sciences, An-Najah National University, P.O. Box 7, 00970, Nablus, Palestine
Johnny Amer, Ahmed Mousa: Department of Biomedical Sciences, Physiology, Pharmacology & Toxicology Division, Faculty of Medicine and Health Sciences, An-Najah National University, Nablus, Palestine
Serkan Levent: Department of Pharmaceutical Chemistry, Faculty of Pharmacy, Anadolu University, 26470, Eskisehir, Turkey
ORCID: Mohammed Hawash 0000-0001-5640-9700

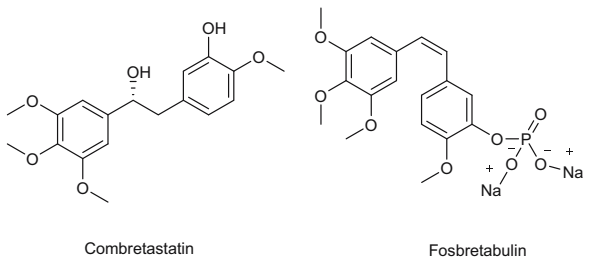

Figure 1: Combretastatin, CA-4P (fosbretabulin) structures.

were extracts from plants with various pharmacological activities [10,11] and some of them with cytotoxic activity [12]. One of the most extracted compounds, the Combretastatin, was isolated from the African *Combretum caffrum* plant and it was successfully modified to find new analogs with potent anticancer activity. In recent years, fosbretabulin (combretastatin A-4 phosphate) (Figure 1) was approved by the FDA and utilized for the treatment of thyroid cancer [13,14].

Many types of research attempt to combine or hybridize various chemical moieties to develop new anticancer agents [15,16]. Many compounds that have halogen-aryl with heterocyclic-carboxamide as a linker with methoxyphenyl were synthesized and evaluated as anticancer agents (st.1, Figure 2), and many other compounds were synthesized, which combined the heterocyclic-carboxamide with the methoxyphenyl moiety (st.2, and st.3; Figure 2) [17]. However, heterocyclic compounds that contain nitrogen with oxygen atoms have diverse medical and biological activities. One of these molecules is the isoxazole ring, which has various biological activities such as anticancer, antituberculosis, insecticidal, antibacterial, and antifungal [5]. Many researchers have focused on this heterocycle (isoxazole) and have synthesized compounds with anticancer activity (st.4, and st.5; Figure 2) [17–20].

Regarding the mentioned data, the current study aims to synthesize novel fluorophenyl-isoxazole-carboxamide analogs with different substituents and evaluate their anticancer activity on various cancer cell lines including, HeLa, MCF-7, HepG2, and HepB3, utilizing different anticancer tests (α-fetoprotein, cell cycle analysis, and apoptosis/necrosis).

2 Experimental

2.1 Materials and chemical methods

2.1.1 Chemical reagents and instruments

All the used chemical reagents were purchased from Alfa Aesar (Massachusetts, United States) and Sigma-Aldrich (Schnelldorf, Germany). SMP-II digital melting point apparatus was used without correction to determine the melting points of the synthesized compounds. Proton and carbon nuclear magnetic resonance (NMR) spectra were recorded in DMSO-d6 and were performed on a Bruker 300 MHz-Avance III High-Performance Digital FT-NMR spectrometer at the Doping and Narcotics Analysis Laboratory in the Faculty of Pharmacy, Anadolu University, Turkey. Tetramethylsilane (TMS) was used as an internal standard. All

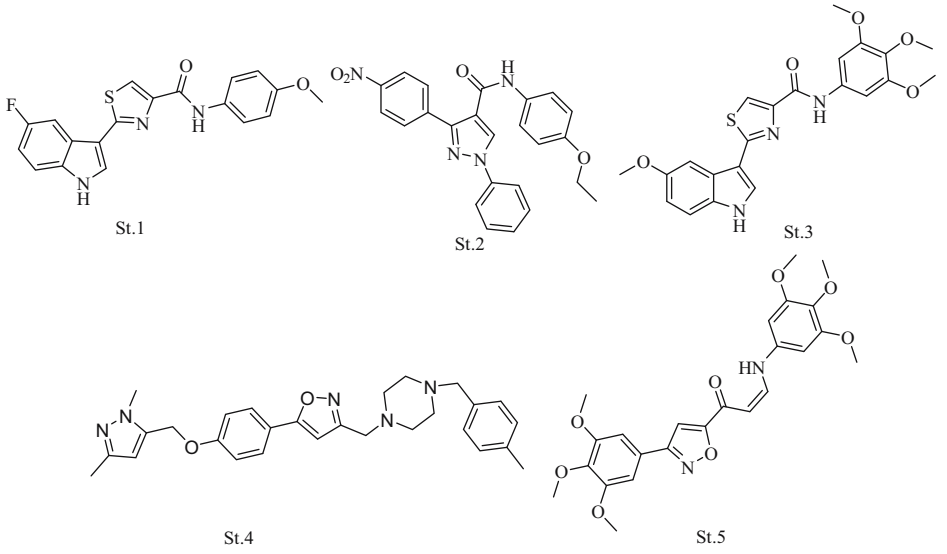

Figure 2: Compounds with fluoro-aryl, heterocyclic-amide, methoxy phenyl, and isoxazole with anticancer activities.

chemical shifts were recorded as δ (ppm). High-resolution mass spectrometer data (HRMS) were collected using a Waters LCT Premier XE Mass Spectrometer (high sensitivity orthogonal acceleration time-of-flight instrument) using ESI (positive proton) method; the instrument is coupled to an ACQUITY Ultra Performance Liquid Chromatography system (Waters Corporation, Milford, MA, USA) at Pharmacy Faculty, of Gazi University, Ankara-Turkey.

2.2 Synthesis

2.2.1 The general synthesis procedure of fluoro-isoxazole-carboxamide derivatives (2a–2f)

15 mL of dichloromethane (DCM) and 3-(4-fluorophenyl)-5-methylisoxazole-4-carboxylic acid (1) (1.5 mmol) were added and dissolved, and then 4-dimethylaminopyridine (DMAP; 0.3 mmol) and 1-ethyl-3-(3-dimethylamino propyl) carbodiimide (EDC; 1.8 mmol) were added and were allowed to stir under argon gas in room temperature (25°C) for 30–60 min. The aniline derivative (1.8 mmol) was added and the mixture was allowed to stir for 24–72 h. During the stirring of the reaction, the TLC was used to monitor the reaction process. The reaction mixture was dried under vacuumed pressure. Recrystallization and flash chromatography were used to purify the final product [21].

2.2.1.1 3-(4-Fluorophenyl)-5-methyl-*N*-(3,4,5-trimethoxyphenyl)isoxazole-4-carboxamide (2a)

This product was purified by column chromatography *n*-hexane:ethyl acetate (1:4) solvent system. Solid product, M.P. 156–158°C. Yield 77%; ESI-MS: 387.1365 (100), 388.1396 (20). For $C_{20}H_{19}FN_2O_5$. IR (FTIR/FTNIR-ATR): 1,699 cm^{-1} amide carbonyl (C═O). ^{1}H NMR (DMSO-d6) δ: 10.42 (1H, s, amide NH), 7.74 (2H, *t*, *J* = 7.35 Hz, Ar-H), 7.36 (2H, *t*, *J* = 9 Hz, Ar-H), 7.01 (2H, s, Ar-H), 3.73 (6H, s, O-CH_3), 3.61 (3H, s, O-CH_3), 2.57 (3H, s, CH_3). ^{13}C NMR (DMSO-d_6) δ ppm: 170.51 (Carbonyl carbone), 165.23, 161.96, 160.15, 159.83, 153.21, 135.17, 130.65, 130.54, 116.61, 116.32, 97.82 (aromatic carbone), 60.55 & 56.16 (methoxy carbone), 12.47 (alphatic carbone).

2.2.1.2 *N*-(4-(*tert*-Butyl)phenyl)-3-(4-fluorophenyl)-5-methylisoxazole-4-carboxamide (2b)

This product was purified by column chromatography DCM:ethyl acetate solvent system (3:2). Solid product, M.P. 169–171°C. Yield 66%; ESI-MS: 353.1665 (100), 354.1721 (20). For $C_{20}H_{21}FN_2O_2$. IR (FTIR/FTNIR-ATR): 1699.19 cm^{-1} amide carbonyl (C═O). ^{1}H NMR (DMSO-d_6) δ: 10.41 (1H, s, amide NH), 7.72–7.77 (2H, m, Ar-H), 7.54 (2H, d, *J* = 8.7 Hz, Ar-H), 7.31–7.37 (4H, m, Ar-H), 2.56 (3H, s, CH_3), 1.25 (9H, s, –C–$(CH_3)_3$). ^{13}C NMR (DMSO-d_6) δ ppm: 170.43 (carbonyl carbone), 165.20, 161.92, 160.12, 159.77, 146.96, 139.41, 136.45, 130.59, 130.47, 125.91, 124.98, 119.91, 116.58, 116.29, 113.71 (aromatic carbone), 31.61 & 12.39 (alphatic carbone).

2.2.1.3 *N*-(4-Chloro-2,5-dimethoxyphenyl)-3-(4-fluorophenyl)-5-methylisoxazole-4-carboxamide (2c)

This product was purified by column chromatography *n*-hexane:ethyl acetate solvent system (3:2). Solid product, M.P. 202–204°C. Yield 82%; ESI-MS: 391.0850 (100), 393.0853 (33). For $C_{19}H_{16}ClFN_2O_4$. IR (FTIR/FTNIR-ATR): 1,716 cm^{-1} amide carbonyl (C═O). ^{1}H NMR (DMSO-d_6) δ: 9.30 (1H, s, amide NH), 7.83 (1H, s, Ar-H), 7.75 (2H, t, *J* = 7 Hz, Ar-H), 7.39 (2H, t, *J* = 9 Hz, Ar-H), 7.15 (1H, s, Ar-H), 3.78 (3H, s, O-CH_3), 3.66 (3H, s, O-CH_3), 2.65 (3H, s, CH_3). ^{13}C NMR (DMSO-d_6) δ ppm: 165.35 (carbonyl carbone), 159.90, 148.53, 131.31, 131.99, 126.44, 124.81, 116.86, 116.61, 116.32, 113.81, 112.81, 112.86, 108.18 (aromatic carbone), 55.93 (methoxy carbone), 12.79 (alphatic carbone).

2.2.1.4 *N*-(3,5-Dimethoxyphenyl)-3-(4-fluorophenyl)-5-methylisoxazole-4-carboxamide (2d)

This product was purified by column chromatography DCM:ethyl acetate solvent system (3:2) and then by recrystallization acetone:water system. Solid product, M.P. 135–137°C, Yield 91%; ESI-MS: 357.1251 (100), 358.1292 (20). For $C_{19}H_{17}FN_2O_4$. IR (FTIR/FTNIR-ATR): 1699.16 cm^{-1} amide carbonyl (C═O). ^{1}H NMR (DMSO-d_6) δ: 10.42 (1H, s, amide NH), 7.73 (2H, t, *J* = 7.2 Hz, Ar-H), 7.35 (2H, t, *J* = 9 Hz, Ar-H), 6.86 (2H, d, *J* = 1.8 Hz, Ar-H), 6.28 (1H, t, *J* = 2.1 Hz, Ar-H), 3.71 (6H, s, O-CH_3), 2.56 (3H, s, CH_3). ^{13}C NMR (DMSO-d_6) δ ppm: 170.60 (carbonyl carbone), 165.24, 161.96, 160.97, 159.84, 140.64, 130.64, 130.53, 124.98, 116.62, 116.33, 113.67, 98.74, 96.43 (aromatic carbone), 55.62 & 55.59 (methoxy carbone), 12.47 (alphatic carbone).

2.2.1.5 *N*-(3,4-Dimethoxyphenyl)-3-(4-fluorophenyl)-5-methylisoxazole-4-carboxamide (2e)

This product was purified by column chromatography DCM:ethyl acetate solvent system (2.5:2.5). Solid product,

M.P. 171–172.5°C. Yield 90%; ESI-MS: 357.1252 (100), 358.1289 (20). For $C_{19}H_{17}FN_2O_4$. IR (FTIR/FTNIR-ATR): 1,683 cm^{-1} amide carbonyl (C═O). ^1H NMR (DMSO-d_6) δ: 10.33 (1H, s, amide NH), 7.75 (2H, t, J = 7 Hz, Ar-H), 7.31–7.38 (3H, m, Ar-H), 7.13 (1H, dd, J = 8.7, 2.4 Hz, Ar-H), 6.91 (1H, d, J = 8.7 Hz, Ar-H), 3.72 (6H, s, O-CH_3), 2.57 (3H, s, CH_3). ^{13}C NMR (DMSO-d_6) δ ppm: 170.39 (carbonyl carbone), 165.22, 159.88, 159.82, 148.96, 145.89, 132.54, 130.65, 130.53, 116.59, 116.30, 112.37, 112.13, 105.10 (aromatic carbone), 56.14, 55.82 (methoxy carbone), 12.45 (alphatic carbone).

2.2.1.6 3-(4-Fluorophenyl)-5-methyl-*N*-phenylisoxazole-4-carboxamide (2f)

This product was purified by column chromatography DCM:ethyl acetate solvent system (3.5:1.5). Solid product, M.P. 149–150.5°C. Yield 89%; IR (FTIR/FTNIR-ATR): 1,684 cm^{-1} amide carbonyl (C═O). ^1H NMR (DMSO-d_6) δ: 10.47 (1H, s, amide NH), 7.73–7.77 (2H, m, Ar-H), 7.62 (2H, d, J = 7.5 Hz, Ar-H), 7.32–7.38 (4H, m, Ar-H), 7.11 (1H, t, J = 7.2 Hz, Ar-H), 2.58 (3H, s, CH_3). ^{13}C NMR (DMSO-d_6) δ ppm: 170.55 (carbonyl carbone), 165.21, 161.94, 160.92, 159.82, 139.01, 130.63, 130.52, 129.29, 124.96, 124.57, 120.20, 116.58, 116.29, 113.67, 99.97 (aromatic carbone), 12.44 (alphatic carbone).

2.3 Chemo-informatics properties of synthesized compounds

Regarding the basis of Lipinski's rule of five (RO5) and chemo-informatics properties, the synthesized compounds were evaluated and multiple online servers were employed, such as Molsoft (http://www.molsoft.com/) and Molinspiration (http://www.molinspiration.com/), to predict the bioactivity score and molecular properties of newly designed compounds.

2.4 Biological methods

Cell culture, MTS assay, apoptosis, α-fetoprotein, cell cycle, and flow cytometry.

HCC (Hep3B and HepG2), cervical adenocarcinoma (HeLa), and breast carcinoma (MCF7) were used as cancer cell lines which were cultured in RPMI-1640 media and accomplished with 10% fetal bovine serum, 1% L-glutamine, and 1% penicillin/streptomycin antibiotics. Then, the cells were matured in a moist atmosphere with 5% CO_2 at 37°C. In a 96-well plate, the cells were seeded at 2.6 × 104 cells/well. After 72 h, the cells were confluent and media was changed and then the cells were incubated with various concentrations (500, 100, 50, 10, and 1 µg/mL) of the evaluated compounds (**2a–2f**) for 24 h. The viability of cells was assessed by Cell Tilter 96® Aqueous One Solution Cell Proliferation (MTS) Assay regarding the manufacturer's procedures (Promega Corporation, Madison, WI). However, at the end of the treatment, about 20 µL/100 µL of MTS solution/media was added to each well, and for 2 h, they were incubated at 37°C. Finally, the absorbance was measured at 490 nm [22].

DMEM was applied to culture Hep3B, using a serum of 10% fetal bovine and we detect tumor activity by using α-FP (α-fetoprotein) as a marker. We indicate Hep3B cell by smearing HBsAg on its surface (Water et al., 1998). Hep3B was incubated with each compound in 10 µl/mL for 24 h. After that, a commercially obtainable ELISA kit from R & D Systems, Inc., USA, was used to assess the level of α-FP in the medium, then harvested, and trypsinized the Hep3B cells (0.05% trypsin/0.53 Mm EDTA); after that, was washed and finally analyzed for cell cycle and apoptosis by the mechanism of flow cytometry.

After Hep3B cells were harvested, they were adjusted to 10^6/mL buffer (in saline containing 1% albumin: the biological industries, Israel) for 10 min to found out their purity, which has staining properties, considering they were fixed with 4% paraformaldehyde. After that, for 20 min, cells were permeabilized with 0.1% saponin in PBS, then, for 30 min, stained using antihuman HBsAg monoclonal antibody (R&D system, USA), all at room temperature. After that, according to manufacture direction, we made apoptosis and viability measurements, by staining fragmented DNA using propidium-iodide PI, while annexin V-conjugated to FITC to stain phosphatidylserine (R&D systems, Minneapolis, Mn) [23].

Annexin-V (+) and propidium-iodide (–) define apoptosis, while annexin-V (–) and propidium-iodide (–) indicate the presence of viable cell. In each experimental test, unstained controls were used, such as FMO and IgG isotypes. Propidium-iodide was utilized to analyze the cell cycle by quantitation of the contents of DNA. Seventy percent of cold ethanol at 40 C was added to fixed Hep3B for 30 min at least, then the cell was washed 2 times using PBS. Finally, discard the supernatant after Rotate at 2,000 rpm. To make sure that DNA was exclusively stained, we treated the cells with ribonuclease (50 mcg of 100 mcg/mL RNase), and then 5 mcL of 50 mcg propidium-iodide/100 mL was applied to stain them; after that flow cytometer was used as an analyzer (Becton-Dickinson LSR 11, Immunofluorometry systems, Mountain View, CA).

According to the manufacturer's procedures, the apoptosis and viability analyses were done, and the used staining was the phosphatidylserine staining by annexin V-conjugated to FITC and propidium-iodide staining of DNA fragments (R&D Systems, Minneapolis, MN). Viable cells were specified as negative for both annexin-V and propidium-iodide (–), while the apoptosis was specified as negative for propidium-iodide (–) and as positive for annexin-V (+). In each experimental tuning, unstained controls were used, such as those mentioned before (FMO and IgG isotype) [24].

Cell cycle test was processed by using propidium-iodide to quantitate the DNA contents. The Hep3B cells were settled in cold 70% of ethanol for at least 30 min at 4°C and then the cells were washed twice in PBS. Spin at 2,000 rpm and the supernatant was discarded. To be sure that just DNA is stained, the treatment with ribonuclease (50 µL of 100 µg/mL RNase) was performed on the cells, and then stained with 5 µL of 50 µg of propidium-iodide/100 mL, and by the flow cytometer (Becton-Dickinson LSR II, Immunofluorometry systems, Mountain View, CA), was measured [24].

Hep3B, HeLa, and MCF7 cancer cell lines were cultured in Roswell Park Memorial Institute (RPMI)-1640 medium and supplemented with 10% fetal bovine serum, 1% L-glutamine, and 1% penicillin/streptomycin in a humidified atmosphere with 5% CO_2 at 37°C. The cells were seeded at 2.6×10^4 cells/well in a 96-well plate. After 72 h, the cells were confluent; the medium was changed and cells were incubated with various concentrations (500, 100, 50, 10, and 1 µg/mL) of the synthesized compounds for 24 h. Cell viability was assessed with the Cell Tilter 96® Aqueous One Solution Cell Proliferation (MTS) assay according to the manufacturer's instructions (Promega Corporation, Madison, WI). Briefly, at the end of the treatment, 20 µL of MTS solution per 100 µL of the medium was added to each well and incubated at 37°C for 2 h. The absorbance was measured at 490 nm [25].

Ethical approval: The conducted research is not related to either human or animal use.

3 Results and discussion

3.1 Chemistry

The synthesis of novel fluorophenyl-isoxazole-carboxamide derivatives (**2a–2f**) was outlined in Scheme 1. The coupling reaction to form the fluorophenyl-isoxazole-carboxamide compounds **2a–2f** was afforded by using EDCI and DMAP as activating agent and covalent nucleophilic catalysts, respectively. After the coupling step, they were reacted with the aniline derivatives [26], EDCI (1-ethyl-3-(30-dimethylamino)carbodiimide, and are usually used for peptide or amide coupling, and there is no need for additional amine. The carbodiimide reacts with the COOH (carboxylic acid) to form the anhydride mixed with O-acylisourea; the produced intermediate directly reacts with the aniline or amine derivatives to produce the desired final amide product as well as urea as side-product [27]. The synthesis of these derivatives was confirmed HRMS, the ppm values for all compounds were less than 2.8, the difference between the calculated mass and the founded mass for all compounds was less than 0.0011 g/mol, for example, compound **2a's** calculated mass was 387.1356 g/mol in comparison with founded mass 387.1265 g/mol. Further, they were purified by column chromatography using different solvent systems (*n*-hexane: ethyl acetate, and dichloromethane: ethyl acetate). The ^{1}H-NMR peaks confirmed the synthesis of these products. A singlet peak of one proton for N–H amide in the range of 9.30–10.47 ppm was observed in each compound. Multiple signals in the aromatic region were observed, and singlet peaks integrated for 3 protons were observed around 2.60 ppm which refers to the methyl group on the isoxazole ring. The ^{13}C-NMR spectrum showed a C signal of carbonyl around 170.5 ppm, and at 12.5 ppm, the signal of aliphatic carbon methyl.

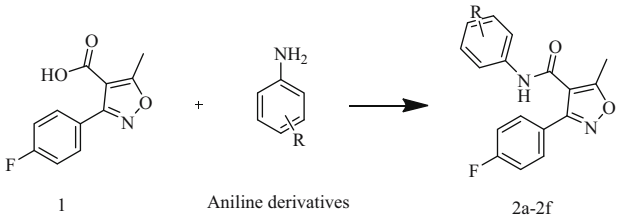

Scheme 1: 1+ aniline derivatives stirred in 16 mL DCM, then DMAP and EDC were added under inert gas and stirred for 24–48 h.

3.2 LO5 and chemo-informatics properties of synthesized compounds (2a–2f)

The predicted chemo-informatic characteristics were processed by computational tools. Results showed that synthesized compounds **2a–2f** have excellent predicted values regarding the molecular weight (g/mol), hydrogen bond acceptor and donor (HBA & HBD, respectively), partition coefficient (log *P*), the polar surface area (PSA; A2), and molar volume (M.V.; A3). Moreover, the RO5 analysis depicted that almost all synthesized compounds,

Table 1: Chemo-informatics properties of synthesized compounds **2a–2f**

Properties	2a	2b	2c	2d	2e	2f	Standard
M.Wt (g/mol)	386.13	352.16	390.08	356.12	356.12	296.10	<500
HBA	7	4	6	6	6	4	<10
HBD	1	1	1	1	1	1	<5
log *P*	2.84	5.08	3.89	3.54	2.87	3.15	<5
PSA (A^2)	68.27	45.29	59.85	60.38	60.55	45.29	<89
nrotb	6	4	5	5	5	3	<10
Drug score	0.95	0.67	0.77	0.84	0.46	0.85	0.0–2.0

2a–2f, obey this rule and possess excellent values regarding the standard values (Table 1) [28]. Our predicted data showed that all synthesized compounds were within the standard range, which showed their good oral bioavailability character. However, drug score parameter was used to evaluate the synthesized compounds according to their hydrogen bonding properties, molecule size, hydrophobicity, flexibility, and electronic distribution and the results showed that all the synthesized structures showed excellent drug score values (0.45–0.95), which represents its better drug-likeness behavior and may be assumed as drug candidate agents against their targets. The overall predicted values of all synthesized compounds are listed in Table 1.

3.3 Biological evaluations

3.3.1 Cytotoxic evaluation of the compounds 2a–2f

The MTS test was utilized on MCF-7, HeLa, Hep3B, and HepG2 cancer cell lines to assess the cytotoxicity of the produced new compounds. As shown in Table 2, five concentrations were used (500, 100, 50, 10, and 1 μg/mL). Based on the results shown in Table 2, the compound **2f** showed the most potent activity on Hep3B and HepG2 cancer cell lines, with IC_{50} values of 5.76 and 34.64 μg/mL, respectively, while compounds **2a–2c** and **2e** showed IC_{50} values below 11.6 μg/mL against the Hep3B cancer cell line. However,

Table 2: IC_{50} of fluorophenyl-isoxazole-carboxamide compounds and doxorubicin on different cancer cells (Hep3B, HepG2, Hela, and MCF-7)

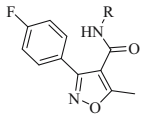

		IC_{50} (μg/mL)			
Code	**R group**	**Hep 3B**	**HepG2**	**HeLa**	**MCF-7**
2a	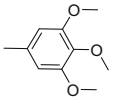	11.6 ± 1.4	>100	59.48 ± 2.1	>100
2b	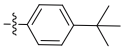	9.58 ± 1.2	41.53 ± 2.3	>100	>100
2c	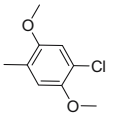	8.54 ± 1.7	38.85 ± 2.6	61.99 ± 2.7	81.96 ± 3.1
2d	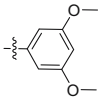	89.12 ± 3.6	48.50 ± 3.5	>100	>100
2e	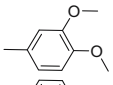	7.66 ± 1.2	44.98 ± 2.1	>100	>100
2f		5.76 ± 1.1	34.64 ± 2.4	90.12 ± 2.3	>100
DOX		1.21 ± 1.0	1.59 ± 0.9	0.84 ± 1.1	3.19 ± 1.3

Note: *P* value ≤0.05.

compounds **2b–2e** showed moderate activities against HepG2 with IC_{50} values in the range of 38.8–48.5 μg/mL. In contrast, our synthesized compounds showed weak or negligible activities against HeLa and MCF7 cancer cell lines with IC_{50} values over 51 μg/mL. Previously, our research group was synthesized in a similar series of chlorophenyl isoxazole derivatives, and the halogen (Cl) was on the ortho position on the phenyl ring; the most active compound was 3-(2-chlorophenyl)-*N*-(3,4-dimethoxyphenyl)-5-methylisoxazole-4-carboxamide against Hep3B with IC_{50} value of 23 μg/mL [21]. However, in this current series, the same compound with fluorophenyl showed better activities against Hep3B with IC_{50} 7.66 μg/mL, as well as almost all of these new series compounds were more potent than the previous work.

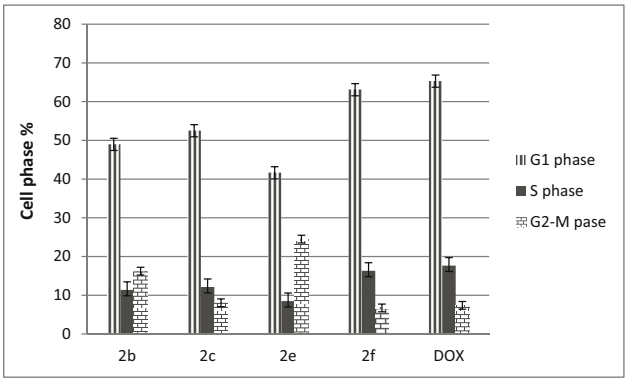

Figure 4: Cell cycle analysis of Hep3B cells after treatment with the synthesized compounds and DOX.

3.3.2 Alpha-fetoprotein results

According to the results of the MTS test and because the synthesized compounds showed potent activities against Hep3B, the inhibitory effects on cell proliferation were used and medium levels of *α*-FP were evaluated. Actually, all synthesized compounds, except the **2d** compound, showed a reduction of secretion with values below 598 ng/mL. The compound **2f** was the most active compound in the MTS assay and decreased the Hep3B secretions of *α*-FP to 168.33 ng/mL in comparison with untreated cells with a value of 1116.67 ng/mL. The results showed that the **2f** compound has anticancer activity on the Hep3B cancer cell line (Figure 3).

3.3.3 Cell cycle analysis of Hep3B cells

The flow cytometry analysis was used to verify the ability of **2f** and other active compounds (**2b**, **2c**, and **2e**) in changing the behaviors for each phase in the cell cycle of Hep3B cell lines. These changes of the normal disturbances in the cell cycle phases were investigated using the boiled solution of the active derivatives to induce cell cycle progression, and they were compared with positive control anticancer drug doxorubicin (Dox). The data in Figure 4 show a similar proportion of cells in the G1 phase following treatment with **2f** compound as compared with DOX. The **2f** compound showed also similar behaviors as the DOX in reducing proportions of cell percentages in the S, as well as the G2-M phase ($P < 0.05$). These data showed significant changes in cell cycle parameters in different phases, especially in S and the G2/M phase (mitosis state); these results indicate a significant delay in the mitotic phase and can confirm the potent anticancer activity of the **2f** compound.

3.3.4 Apoptosis versus necrosis test

The next step of the current study was to determine whether the synthesized compounds induced programmed

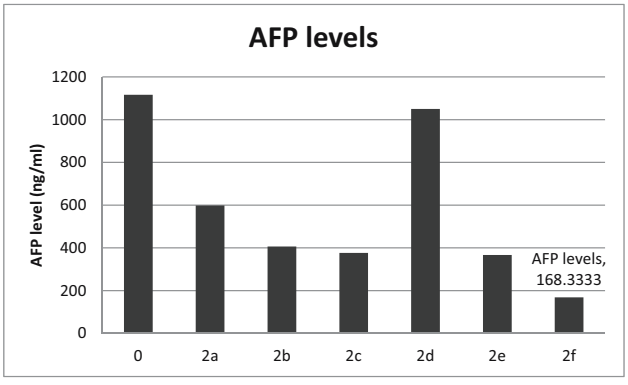

Figure 3: Cell proliferation of the synthesized compound **2a–2f** and untreated cells (control).

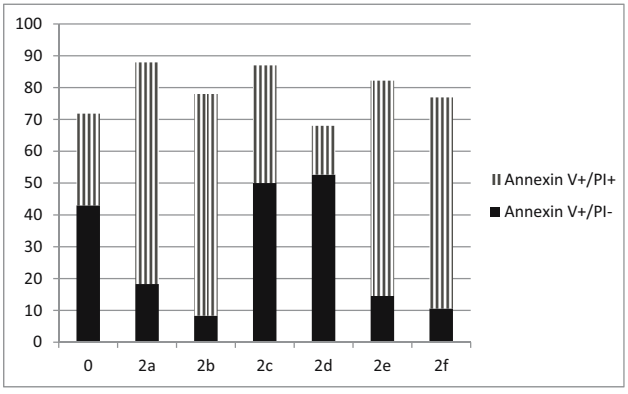

Figure 5: Necrosis versus apoptosis of the synthesized compounds.

cell death (apoptosis) and necrosis. Apoptosis was defined as AnnexivV+/PI–, while late apoptotic or necrotic cells were defined as AnnexivV+/PI+. Figure 5 illustrates that Hep3B untreated cells possess a baseline apoptotic cell population of 43.0%, while **2b**, **2e,** and **2f** compounds reduced apoptosis to 8.3, 14.53, and 10.6%, respectively. An annexin-V+/PI+ fraction from **2b**, **2e,** and **2f** compounds significantly increased apoptosis/necrosis cells to 69.67, 67.66, and 66.33%, respectively, as compared with 28.83% in untreated cells. These findings support the 2f compound's potent anticancer properties by increasing the necrotic activity of annexin-V+/PI+ in the Hep3B cell line, thereby hastening their death.

4 Conclusion

The synthesized fluoro-isoxazole-carboxamide derivatives showed anticancer activity on the hepatocellular cancer cell lines. Five compounds showed potent activity against the Hep3B cancer cell line, with IC_{50} values close to the positive control Dox. The most potent compound **2f** demonstrated potent anticancer activity in different *in vitro* tests. The MTS assay showed potent activity against Hep3B, with IC_{50} around 5 μg/mL, moderate activity against HepG2, with IC_{50} values around 35 μg/mL, and weak activity against HeLa, with IC_{50} values around 90 μg/mL. The α-FP tumor marker analysis of **2f** derivative decreased the Hep3B secretions to 168 ng/mL compared with 1,116 ng/mL in the negative control (untreated cells), indicating less proliferation and tumorigenicity of Hep3B. For further evaluation of the molecular effects of the novel synthesized compounds, the **2f** compound induces cell cycle arrest in the mitotic phase (G2/M) and is similar to Dox positive control values. In future projects, further analogs and derivatives based on the lead compound **2f** will be designed and synthesized as promising anticancer agents. More *in vivo* research is needed to confirm the efficacy and create appropriate pharmaceutical dosage forms for the most active substances.

Acknowledgments: The authors would like to thank An-Najah National University and Anadolu University for their support in chemical analysis.

Funding information: Not applicable.

Author contributions: M. H designed the compounds and their synthesis. S.I., S.I., & A.A. performed the chemical synthesis. S.L. & T.S. characterized the compounds. M.H., N.J., & M.A. contributed to the writing of the manuscript. M.H., J.A., & A.M. designed the biological experiments. J.A. & A.M. performed the experiments for biological evaluation of the compounds on cancer cells. All authors have given approval to the final version of the manuscript.

Conflict of interest: The authors state no conflict of interest.

Data availability statement: The datasets used and/or analyzed during the current study are available from the corresponding author on reasonable request.

References

[1] Sekhon R, Bhatla N. Gynecological cancer update. Asian J Oncol. 2016;2(2):61.
[2] Didkowska J, Wojciechowska U, Mańczuk M, Łobaszewski J. Lung cancer epidemiology: contemporary and future challenges worldwide. Ann Transl Med. 2016;4(8):1–11.
[3] Hawash M. Highlights on specific biological targets; cyclin-dependent kinases, epidermal growth factor receptors, ras protein, and cancer stem cells in anticancer drug development. Drug Res. 2019;69(09):471–8.
[4] Fitzmaurice C, Akinyemiju TF, Al Lami FH, Alam T, Alizadeh-Navaei R, Allen C, et al. Global, regional, and national cancer incidence, mortality, years of life lost, years lived with disability, and disability-adjusted life-years for 29 cancer groups, 1990 to 2016: a systematic analysis for the global burden of disease study. JAMA Oncol. 2018;4(11):1553–68.
[5] Kumar KA, Jayaroopa P. Isoxazoles: molecules with potential medicinal properties. Int J Pharm Chem Biol Sci. 2013;3:294–304.
[6] Vilchez V, Turcios L, Marti F, Gedaly R. Targeting Wnt/β-catenin pathway in hepatocellular carcinoma treatment. World J Gastroenterol. 2016;22(2):823.
[7] Sherr CJ. Cancer cell cycles. Science. 1996;274(5293):1672–7.
[8] Sysak A, Obmińska-Mrukowicz B. Isoxazole ring as a useful scaffold in a search for new therapeutic agents. Eur J Med Chem. 2017;137:292–309.
[9] Huang C-Y, Ju D-T, Chang C-F, Reddy PM, Velmurugan BK. A review on the effects of current chemotherapy drugs and natural agents in treating non–small cell lung cancer. Biomedicine. 2017;7(4):12–23.
[10] Jaradat N, Zaid A, Hussein F, Zaqzouq M, Aljammal H, Ayesh O. Anti-lipase potential of the organic and aqueous extracts of ten traditional edible and medicinal plants in Palestine; a comparison study with orlistat. Medicines. 2017;4(4):89.
[11] Jaradat N, Hawash M, Dass G. Phytochemical analysis, in-vitro anti-proliferative, anti-oxidant, anti-diabetic, and anti-obesity activities of Rumex rothschildianus Aarons. extracts. BMC Compl Med Ther. 2021;21(1):1–11.
[12] Jaradat NA, Al-lahham S, Zaid AN, Hussein F, Issa L, Abualhasan MN, et al. Carlina curetum plant

phytoconstituents, enzymes inhibitory and cytotoxic activity on cervical epithelial carcinoma and colon cancer cell lines. Eur J Integr Med. 2019;30:100933.
[13] Abma E, Daminet S, Smets P, Ni Y, de Rooster H. Combretastatin A4-phosphate and its potential in veterinary oncology. Vet Comp Oncol. 2017;15(1):184–93.
[14] Nathan P, Zweifel M, Padhani AR, Koh DM, Ng M, Collins DJ, et al. Phase I trial of combretastatin A4 phosphate (CA4P) in combination with bevacizumab in patients with advanced cancer. Clin Cancer Res. 2012;18(12):1–12.
[15] Kamal A, Reddy VS, Shaik AB, Kumar GB, Vishnuvardhan MV, Polepalli S, et al. Synthesis of (Z)-(arylamino)-pyrazolyl/isoxazolyl-2-propenones as tubulin targeting anticancer agents and apoptotic inducers. Org Biomol Chem. 2015;13(11):3416–31.
[16] Kamal A, Shaik AB, Jain N, Kishor C, Nagabhushana A, Supriya B, et al. Design and synthesis of pyrazole-oxindole conjugates targeting tubulin polymerization as new anticancer agents. Eur J Med Chem. 2015;92:501–13.
[17] Hawash M, Baytas S. Antiproliferative activities of some biologically important scaffold. FABAD J Pharm Sci. 2017;43(1):59–77.
[18] Yong J-P, Lu C-Z, Wu X. Potential anticancer agents. I. synthesis of isoxazole moiety containing quinazoline derivatives and preliminarily in vitro anticancer activity. Anti Cancer Agents Medi Chem Anti Cancer Agents. 2015;15(1):131–6.
[19] Kumar RN, Dev GJ, Ravikumar N, Swaroop DK, Debanjan B, Bharath G, et al. Synthesis of novel triazole/isoxazole functionalized 7-(trifluoromethyl) pyrido [2, 3-d] pyrimidine derivatives as promising anticancer and antibacterial agents. Bioorg Med Chem Lett. 2016;26(12):2927–30.
[20] Shahinshavali S, Sreenivasulu R, Guttikonda V, Kolli D, Rao M. Synthesis and anticancer activity of amide derivatives of 1, 2-isoxazole combined 1, 2, 4-thiadiazole. Russ J Gen Chem. 2019;89(2):324–9.
[21] Eid AM, Hawash M, Amer J, Jarrar A, Qadri S, Alnimer I, et al. Synthesis and biological evaluation of novel isoxazole-amide analogues as anticancer and antioxidant agents. BioMed Res Int. 2021;2021:633297.
[22] Shi M, Ho K, Keating A, Shoichet MS. Doxorubicin-conjugated immuno-nanoparticles for intracellular anticancer drug delivery. Adv Funct Mater. 2009;19(11):1689–96.
[23] Hawash M, Qneibi M, Jaradat N, Abualhasan M, Amer J, Amer EH, et al. The impact of filtered water-pipe smoke on healthy versus cancer cells and their neurodegenerative role on AMPA receptor. Drug Chem Toxicol. 2021;1–9. doi: 10.1080/01480545.2021.1935397.
[24] Waters J, Bailey C, Love C, Thomas H. A study of the antigenicity and immunogenicity of a new hepatitis B vaccine using a panel of monoclonal antibodies. J Med Virol. 1998;54(1):1–6.
[25] Hawash M, Eid AM, Jaradat N, Abualhasan M, Amer J, Naser Zaid A, et al. Synthesis and biological evaluation of benzodioxole derivatives as potential anticancer and antioxidant agents. Heterocycl Commun. 2020;26(1):157–67.
[26] Biava M, Battilocchio C, Poce G, Alfonso S, Consalvi S, Di Capua A, et al. Enhancing the pharmacodynamic profile of a class of selective COX-2 inhibiting nitric oxide donors. Bioorg Med Chem J. 2014;22(2):772–86.
[27] Montalbetti, CAGN, Falque, V, Amide. bond formation and peptide coupling. Tetrahedron. 2005;61(46):10827–52.
[28] Jadhav PB, Yadav AR, Gore MG. Concept of drug likeness in pharmaceutical research. Int J Pharm Biol Sci. 2015;6:142–54.